Development 138, 2632 (2011) doi:10.1242/dev.069518

p120 catenin is required for normal renal tubulogenesis and glomerulogenesis

Denise K. Marciano, Paul R. Brakeman, Chao-Zong Lee, Natalie Spivak, Dennis J. Eastburn, David M. Bryant, Gerard M. Beaudoin III, Ilse Hofmann, Keith E. Mostov and Louis F. Reichardt

There was an error published in *Development* **138**, 2099-2109.

Fig. 8 was not corrected before publication. The correct figure appears below.

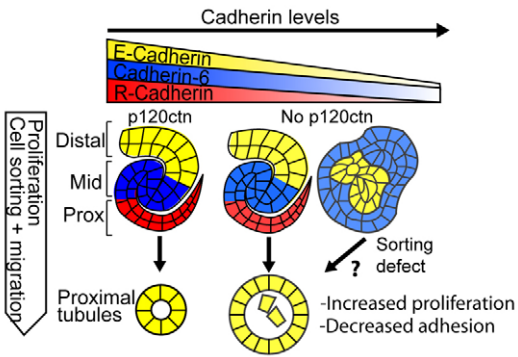

We apologise to the authors and readers for this mistake.

Development 138, 2099-2109 (2011) doi:10.1242/dev.056564

p120 catenin is required for normal renal tubulogenesis and glomerulogenesis

Denise K. Marciano[1,2,*,†], Paul R. Brakeman[3,4], Chao-Zong Lee[1], Natalie Spivak[3,4], Dennis J. Eastburn[4], David M. Bryant[4], Gerard M. Beaudoin III[2], Ilse Hofmann[5], Keith E. Mostov[4] and Louis F. Reichardt[2]

SUMMARY

Defects in the development or maintenance of tubule diameter correlate with polycystic kidney disease. Here, we report that absence of the cadherin regulator p120 catenin (p120ctn) from the renal mesenchyme prior to tubule formation leads to decreased cadherin levels with abnormal morphologies of early tubule structures and developing glomeruli. In addition, mutant mice develop cystic kidney disease, with markedly increased tubule diameter and cellular proliferation, and detached luminal cells only in proximal tubules. The p120ctn homolog Arvcf is specifically absent from embryonic proximal tubules, consistent with the specificity of the proximal tubular phenotype. p120ctn knockdown in renal epithelial cells in 3D culture results in a similar cystic phenotype with reduced levels of E-cadherin and active RhoA. We find that E-cadherin knockdown, but not RhoA inhibition, phenocopies p120ctn knockdown. Taken together, our data show that p120ctn is required for early tubule and glomerular morphogenesis, as well as control of luminal diameter, probably through regulation of cadherins.

KEY WORDS: Cadherins, Glomerulogenesis, Kidney development, p120 catenin, Polycystic disease, Mouse

INTRODUCTION

Kidney development serves as a model for examining the mechanisms that underlie organogenesis, including cellular aggregation, polarization, differentiation and mesenchymal-epithelial interactions. Key processes in kidney development are the formation of tubules and the regulation of their luminal diameters. Abnormal regulation of luminal diameter during development or repair leads to cystic kidney disease (Harris, 2009).

The kidney comprises nephrons and a collecting system, which are derived from the metanephric mesenchyme and ureteric bud, respectively (Dressler, 2009). During development, inductive signals from the mesenchyme cause the ureteric bud to undergo branching, whereas signals from the ureteric bud induce the conversion of mesenchyme to epithelium (Saxen and Sariola, 1987). Mesenchymal conversion occurs via condensation around ureteric bud tips, followed by formation of pre-tubular cell aggregates, which then form polarized epithelial renal vesicles. The renal vesicles elongate into comma-shaped and then s-shaped bodies. Cells in the proximal domain of the s-shaped body differentiate to form the epithelial cells of the renal glomerulus. Cells in the mid- and distal domains differentiate into the tubular portion of the nephron, which is segmented into proximal tubules, loops of Henle and distal tubules.

[1]Department of Medicine, University of California, San Francisco, CA 94158, USA.
[2]Department of Physiology, University of California, San Francisco, CA 94158, USA.
[3]Department of Pediatrics, University of California, San Francisco, CA 94158, USA.
[4]Department of Anatomy, University of California, San Francisco, CA 94158, USA.
[5]Joint Research Division Vascular Biology, Medical Faculty Mannheim, 68167 Mannheim, Germany.

*Present address: Department of Medicine, University of Texas Southwestern Medical Center, Dallas, TX 75390, USA
†Author for correspondence (denise.marciano@utsouthwestern.edu)

Accepted 17 February 2011

The differential expression of cadherins is an early aspect of tubule segmentation in the developing nephron (Cho and Dressler, 2003). Cadherins play crucial roles in tissue morphogenesis, the control of polarity, proliferation, coordinated cell movements, and transitions between cellular states (Gumbiner, 2005; Halbleib and Nelson, 2006). The cytoplasmic domains of cadherins interact with proteins called catenins. Both p120 catenin (p120ctn; Ctnnd1 – Mouse Genome Informatics) and β-catenin (Ctnnb1) bind to distinct regions of the cytoplasmic tails of cadherins and play important roles in organizing the cytoskeleton and regulating cell signaling (Reynolds, 2007).

Cadherins are differentially expressed within subdomains of the developing kidney (Cho and Dressler, 2003; Cho et al., 1998; Dahl et al., 2002). In the ureteric bud, E-cadherin (cadherin 1) is the predominant cadherin. In the adjacent mesenchyme, significant cadherin subtype switching occurs. Cadherin 11 is expressed in the mesenchyme but is downregulated as the mesenchyme epithelializes. As pre-tubular aggregates form, R-cadherin (cadherin 4) and cadherin 6 are upregulated. As the renal vesicle elongates into the comma- and s-shaped body, R-cadherin is expressed in the proximal and mid-regions whereas E-cadherin is expressed distally. Cadherin 6 is expressed in the mid-region with some overlap with both R-cadherin and E-cadherin. Finally, as the s-shaped body elongates and differentiates, E-cadherin becomes the predominant cadherin in the proximal and distal tubules, whereas cadherin 6 is expressed in the loop of Henle and the first portion of the distal tubule.

Despite differential cadherin expression during nephrogenesis, only limited defects are seen in mice lacking single cadherins, perhaps owing to compensation by other cadherins. Mice lacking cadherin 6 or R-cadherin exhibit delayed conversion of mesenchyme to epithelia (Dahl et al., 2002; Mah et al., 2000). R-cadherin-deficient mice also exhibit mild widening of proximal tubule lumens (Dahl et al., 2002).

Although β-catenin is known to have crucial roles in nephrogenesis (Park et al., 2007; Schmidt-Ott and Barasch, 2008), the roles of p120ctn family members are not well

characterized. p120ctn, however, has several essential roles in the embryogenesis of multiple tissues (Davis and Reynolds, 2006; Elia et al., 2006; Oas et al., 2010; Perez-Moreno et al., 2006; Smalley-Freed et al., 2010). The p120ctn family consists of four proteins: p120ctn, Arvcf, and the more distantly related δ-catenin (Ctnnd2 – Mouse Genome Informatics) and p0071 (plakophilin 4) (McCrea and Park, 2007). These proteins stabilize cadherins on the cell surface through inhibition of endocytosis (Chiasson et al., 2009; Xiao et al., 2005). Both δ-catenin and Arvcf can functionally substitute for p120ctn in stabilizing surface E-cadherin in vitro (Davis et al., 2003). To date, p120ctn has been shown to stabilize many classical cadherins, including E-cadherin, R-cadherin, N-cadherin (cadherin 2 – Mouse Genome Informatics), P-cadherin (cadherin 3), VE-cadherin (cadherin 5) and cadherin 11 (Reynolds, 2007).

In addition to interacting with cadherins, p120ctn family members regulate Rho GTPases. In mice, differential splicing generates two major isoforms of p120ctn, isoforms 1 and 3 (Montonen et al., 2001), with isoform 1 inhibiting RhoA (Rhoa) and activating Rac1 and Cdc42 (Anastasiadis et al., 2000; Noren et al., 2000; Yanagisawa et al., 2008). Furthermore, Rac1 activation results in RhoA inhibition through a p120ctn-dependent p190RhoGAP (Grlf1) pathway (Wildenberg et al., 2006).

Given p120ctn's ability to regulate multiple cadherins, we postulated that loss of p120ctn would lead to renal defects not observed in the absence of individual cadherins. Thus, we examined deficits following specific deletion of p120ctn in the ureteric bud or metanephric mesenchyme. Surprisingly, p120ctn deletion from ureteric bud resulted in no obvious phenotype. Deletion from metanephric mesenchyme, however, resulted in renal hypoplasia, early defects in tubule morphology, and renal cysts in proximal tubules, concurrent with dramatic reductions in cadherin levels. Glomeruli were abnormal in morphology, displaying deficits in podocyte and endothelial cell organization. Further, p120ctn knockdown in 3D MDCK cell culture led to a similar cystic phenotype with reduced levels of E-cadherin and active RhoA. Knockdown of E-cadherin, but not inhibition of RhoA, phenocopied p120ctn knockdown in cysts. Taken together, our data show that p120ctn is required for tubule and glomerular formation, probably through control of cadherin levels.

MATERIALS AND METHODS

Animals

We crossed *Ctnnd1*$^{flox/flox}$ (floxed p120ctn) females to *Ctnnd1*$^{flox/+}$*;Pax3-cre*$^{tg/+}$ males (Elia et al., 2006; Li et al., 2000) to obtain *Ctnnd1*$^{flox/flox}$*;Pax3-cre*$^{tg/+}$ mutant embryos or pups. Using the same strategy, we generated *Ctnnd1*$^{flox/flox}$*;HoxB7-cre*$^{tg/+}$ pups (Srinivas et al., 1999). Mice were maintained on mixed genetic backgrounds and genotyped by PCR. Procedures were performed according to UCSF IACUC-approved guidelines.

Histology and immunofluorescence

For paraffin sections, embryonic and neonatal kidneys were fixed in 4% paraformaldehyde in PBS, embedded in paraffin and sectioned at 5 μm. For adult kidneys, mice were perfused with 4% paraformaldehyde in PBS. Antigen retrieval was performed on paraffin sections with Trilogy (Cell Marque). Vibratome sections (70 μm) and cryosections (10 μm) were permeabilized with 0.3% Triton X-100 in PBS (PBST) and blocked with 10% donkey sera in PBST. Sections were incubated with primary antibodies overnight at 4°C, then with fluorophore-conjugated secondary antibodies (Invitrogen) and mounted with Prolong Gold (Invitrogen).

Antibodies

Antibodies used were: pp120 (1:1000; BD Transduction, 2B12), p120 NT (1:1000; Invitrogen, 6H11), p120 F1SH (1:1000; a gift from Al Reynolds, Vanderbilt University, TN, USA), Arvcf (1:100) (Walter et al., 2008), E-cadherin (1:1000; ECCD2), cytokeratin 8 (1:50; Developmental Studies Hybridoma bank, TROMA1), cadherin 6 (1:1000; a gift from G. Dressler, University of Michigan, MI, USA), cadherin 6 (1:1000; a gift from J. Nelson, Stanford University, CA, USA), cadherin 11 (1:100; Zymed, 71-7600), NCAM (1:100; 5B8 a gift from T. Jessell, Columbia University, NY, USA), Na/K ATPase (1:500; 5, a gift from M. Caplan, Yale University, CT, USA), calbindin (1:500; Swant, CB-38a), ZO1 (1:100; a gift from B. Stevenson, University of Alberta, Canada), nephrin (1:150; R&D, AF3159), Ki67 (1:200; Vector, VR-RM04), cleaved caspase 3 (1:100; Cell Signaling, 9601), Tamm Horsfall Glycoprotein (1:250; Biogenesis, 8595-0054), NaCl co-transporter (1:500; Chemicon, AB3553), δ-catenin (1:100; BD transduction, 611536), PECAM (1:200; ParMingen Int, 1951A), α-E-catenin (1:1000; Sigma, C8114), active-β-catenin (1:1000; Millipore, 8E7), β-catenin (1:1000; Zymed, 13-8400), R-cadherin (1:1000; BD transduction, 610414). R-cadherin (1:10; MRCD5, Developmental Studies Hybridoma Bank), phosphohistone 3 (1:200; Upstate Cell Signaling, 06-570), acetylated tubulin (1:1000; Sigma, 6-11B-1), RhoA (1:250; SCBT, clone 26C4), aquaporin-2 (1:100; SCBT 9882), laminin (1:200; Sigma, #9393), podocin (1:100; a gift from P. Mundel, Albert Einstein College of Medicine, NY, USA), podocalyxin (1:40; Pcx, R&D systems MAB1556) and phalloidin 488 (1:200, Invitrogen).

Imaging and statistical analysis

Confocal imaging was performed on a Zeiss LSM5 Pascal microscope. Light and immunofluorescence microscopy were performed with a Nikon Eclipse E600 (Axiovision HRc camera and Release 4.6 software) or a Zeiss Axiovert 200M (Slidebook 4.2 software from Intelligent Imaging). Images were analyzed using ImageJ software as indicated. Images were minimally processed with Adobe Photoshop. All data shown are mean ± s.d. Statistical significance was performed using a two-tailed nonparametric Mann-Whitney *U*-test or two-tailed Student's *t*-test.

Western blots

E17.5 mouse kidneys were dissected and homogenized in ice cold buffer containing 1% NP-40, 0.5% sodium deoxycholate, 0.1% SDS, 20 mM sodium phosphate (pH 7.2), 150 mM NaCl, 2 mM Na^+EDTA, 50 mM NaF, 1 mM Na_3VO_4, 1 mM PMSF and a protease inhibitor cocktail (Roche). Lysates were centrifuged at 17,000 ***g*** for 15 minutes at 4°C to remove insoluble aggregates, and SDS-PAGE and western blotting were performed. Densitometric quantification was performed with Image J and normalized to GAPDH.

MDCK culture and shRNA knockdown

MDCK type II cells were grown and imaged as described previously (Brakeman et al., 2009). Briefly, MDCK cells were trypsinized 1 day before plating. On the day of plating, wells were coated with Matrigel (BD Biosciences). Cells were trypsinized and resuspended into a single-cell suspension containing media and 2% Matrigel prior to plating. Cysts were harvested at day five. The shRNA oligos were designed against canine p120 (XM_854180) using the iRNAi program (http://www.mekentosj.com/science/irnai) using guidelines from the Addgene pLKO.1 protocol (www.addgene.org). p120ctn shRNA1 (KD1), CCGGTGACAAGGTGAAGACTGATTTCAAGAGAATCAGTCTTCA-CCTTGTCATTTTTG; p120ctn shRNA2 (KD2), CCGGG-CTGGTGTTGATCAACAAATTCAAGAGATTTGTTGATCAACACC-AGCTTTTTG; E-cadherin shRNA1 (KD1), CCGGGG-ACGTGGAAGATGTGAATCTCGAGATTCACATCTTCCACGTCCT-TTTTG; and E-cadherin shRNA2 (KD2), CCGGGTC-TAACAGGGACAAAGAACTCGAGTTCTTTGTCCCTGTTAGACT-TTTTG were adopted for pLKO.1 (Capaldo and Macara, 2007). shRNAs were cloned into pLKO.1 puro or blast. Viral transduction of MDCK cells was performed as described previously (Bryant et al., 2010).

Measurements of luminal cells and cyst area

To quantify luminal cells, control and p120ctn shRNA cysts were visualized by differential interference contrast (DIC) and immunofluorescence staining. To confirm that intraluminal cells were not attached to the cyst wall, cysts were optically sectioned via confocal microscopy. Cysts with a single lumen (as seen by apical marker podocalyxin staining) were scored for empty lumens or lumens containing ≥1 cell. To measure cyst area, we took automated images of cysts on an IN Cell Analyzer 1000 (GE Healthcare) and converted the images to binary with ImageJ. The cyst outlines were filled and area computed using ImageJ. Cysts contacting other cysts or located at the image border were excluded. The upper quartile of tabulated cyst areas were compared.

Measurements of spindle orientation

Immunofluorescence was performed with α-tubulin, Hoescht and podocalyxin to visualize spindles, nuclei and apical membranes of cysts, respectively. Cysts were imaged by confocal microscopy at the largest cross-sectional diameter (equatorial plane). Spindle orientation parallel to the apical membrane is 0° and perpendicular to the apical membrane is 90°.

Active Rho assays

MDCK cells were lysed in ice cold buffer containing 25 mM Tris-HCl pH 7.5, 150 mM NaCl, 10 mM $MgCl_2$, 1% NP-40, 5% glycerol, 1 mM PMSF and protease inhibitor cocktail. Cells were centrifuged to remove insoluble aggregates. Protein concentration was determined by SDS-PAGE and blot with GAPDH using the Odyssey Infrared Imaging System (Li-Cor Biosciences). Equivalent protein amounts were incubated with 20 μg RBD-GST coupled to glutathione-coupled agarose beads (Cytoskeleton Inc.) for 1 hour at 4°C. After washing, bound material was eluted with Laemmli buffer. Samples were analyzed by blot with anti-RhoA and densitometry.

RESULTS

p120ctn is widely expressed in the developing kidney

p120ctn is widely expressed in many tissues, including adult rat kidney where it localizes to proximal tubules, thick ascending limbs, distal tubules, collecting ducts and developing glomeruli (Golenhofen and Drenckhahn, 2000; Usui et al., 2003). We analyzed the distribution and isoform expression of p120ctn by examining sections of embryonic day (E)17.5 kidney, which contain nephrons at all stages of development.

Western blot analysis identified two p120ctn isoforms in E17.5 kidney lysates (Fig. 1A), isoform 1 and presumptive isoform 3, which is similar to p120ctn isoform expression in other murine tissues (Montonen et al., 2001). Immunofluorescence showed that p120ctn is broadly expressed in uncondensed mesenchyme, condensed mesenchyme and ureteric bud, with highest levels in ureteric bud (Fig. 1C-E). A schematic of the developing renal segments is depicted in Fig. 1B. p120ctn was also present in derivatives of condensed mesenchyme, including renal vesicles (Fig. 1C), comma-shaped bodies (Fig. 1I) and s-shaped bodies (Fig. 1J). Immunofluorescence with the isoform 1-specific antibody demonstrated that p120ctn isoform 1 is also broadly expressed, albeit at much lower levels in ureteric epithelia than condensed mesenchyme (Fig. 1K,L). Isoform 1 levels decreased as mesenchymal-to-epithelial conversion proceeded, with abundant isoform 1 in condensed mesenchyme and lower levels in renal vesicles, comma bodies (Fig. 1K) and s-shaped bodies (not shown). Very little isoform 1 was detected in proximal tubules (Fig. 1M). Cell culture studies have also shown that isoforms 1 and 3 are expressed largely in mesenchymal and epithelial cell lines, respectively (Aho et al., 2002; Keirsebilck et al., 1998; Mo and Reynolds, 1996).

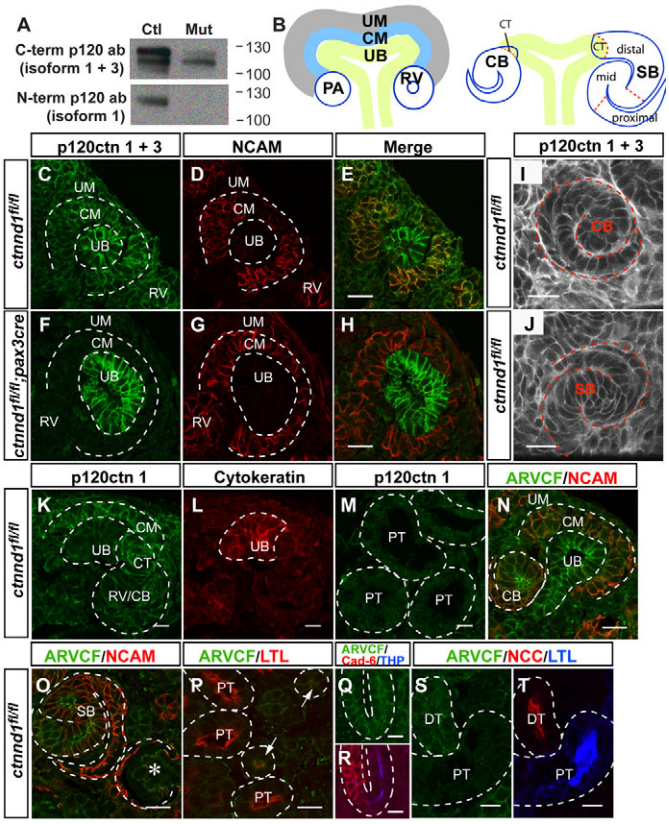

Fig. 1. p120ctn and Arvcf are broadly expressed during metanephric development. (**A**) Western blot of E17.5 kidney lysates in control (Ctl; *ctnnd1*$^{flox/flox}$) and mutant (Mut; *ctnnd1*$^{flox/flox}$; *pax3-cre*$^{tg/0}$) mice with anti-p120ctn mAb pp120 (2B12; anti-p120ctn C-terminus) shows two isoforms. Western blot with anti-p120ctn isoform 1 (6H11, N-terminus mAb) identifies the higher molecular weight band as isoform 1. The lower molecular weight band co-migrates with p120ctn from MDCK cells, which express only isoform 3 (Ohkubo and Ozawa, 2004). (**B**) Schematic of renal development. The ureteric bud (UB) is surrounded by condensed (CM) and uncondensed (UM) mesenchyme. CM differentiates to form pre-tubular aggregates (PA), which epithelialize to form renal vesicles (RV). These lengthen into comma-shaped bodies (CB) and subsequently s-shaped bodies (SB). The connecting tubule (CT) of the UB fuses with the SB to form a continuous lumen. (**C-H**) Localization of p120ctn in E17.5 control shows that p120ctn (green) is present in UM, CM and UB, and the CM derivative RV (C-E). Mutant kidneys lack p120ctn in UM and CM (F-H). NCAM (red) identifies CM, RV, CB and SB. (**I**,**J**) Expression of p120ctn in the CM derivatives CB (I) and SB (J). (**K-M**) Downregulation of p120ctn isoform 1 during mesenchymal-to-epithelial differentiation. (K,L) Localization of p120ctn isoform 1 (mAb 6H11) (green) and cytokeratin (red), a UB marker, at E17.5. Low isoform 1 levels are present in UB compared with CM. Note high isoform 1 in connecting tubules (CT). (M) There is minimal isoform 1 expression in proximal tubules (PT), identified with lotus tetragonolobus lectin (LTL, not shown). (**N-P**) Arvcf expression at E17.5. (N-O) Arvcf (green) is expressed in UB, RV (not shown), CB, SB and a developing glomerulus (asterisk, O). (P) Localization of Arvcf (green) and LTL (red) shows little Arvcf is present in mature PT. Tubules with low LTL (arrows) express Arvcf and might be immature PT or descending loops of Henle. (**Q**,**R**) Arvcf is present in a short loop of Henle, as identified by cadherin 6 (red) and Tamm Horsfall protein (THP, blue). (**S**,**T**) Arvcf is present in a distal tubule (DT), identified by the sodium chloride co-transporter (NCC), but not an adjacent PT (LTL, blue). White and red dotted lines delineate structures. Scale bars: 10 μm in I-M,Q-T; 20 μm in C-H,N-P.

Conditional deletion of p120ctn from renal mesenchyme leads to hypoplastic cystic kidneys

To investigate the functions of p120ctn during nephrogenesis, we deleted the p120ctn gene (*Ctnnd1*) in ureteric bud and metanephric mesenchyme using *HoxB7-cre* and *Pax3-cre*, respectively (Li et al., 2000; Yu et al., 2002). Deletion from ureteric bud did not induce obvious defects in kidney size or morphology at 4 weeks of age, despite efficient deletion of p120ctn (see Fig. S1 in the supplementary material). These mice appeared healthy and were fertile.

Pax3-cre has been shown to induce early and efficient recombination in the metanephric mesenchyme and its epithelial derivatives, including all segments of the nephron (Cheng et al., 2007; Grieshammer et al., 2005). Staining of *Ctnnd1*$^{flox/flox}$; *Pax3-cre*$^{tg/0}$ (hereafter p120ctn mutant) kidneys, showed that p120ctn is absent in uncondensed and condensed mesenchyme (Fig. 1F-H) and its derivatives (data not shown). In these kidneys, western blots showed reduced expression of both isoforms, with almost total elimination of isoform 1 (Fig. 1A).

Late embryonic p120ctn mutants were present at near Mendelian ratios (20%, 27 of 134 embryos at E17.5). Pups were born at similar ratios, but p120ctn mutant pups died within 24 hours. Gross anatomical dissection revealed that the mice produced urine (data not shown), but had significantly smaller kidneys than those of control littermates at E17.5 (data not shown) and P0 (Fig. 2A-D).

Postnatal day (P)0 p120ctn mutant kidneys exhibited normal corticomedullary differentiation (Fig. 2F,G). All elements of the nephron were present, including the proximal tubule (Fig. 3B,D), thick ascending limb (Fig. 3J), distal tubule (Fig. 3H) and glomerulus (see below). Heterozygous and wild-type kidneys were indistinguishable from each other (data not shown). Cystic structures in the P0 p120ctn mutant kidneys were readily apparent with 100% penetrance (27/27) (Fig. 2F,G, arrow). At high magnification the eosinophilic appearance of cysts by Hematoxylin and Eosin (H&E) staining suggests a proximal tubule origin (Fig. 2J,K). In addition, nuclear crowding (compare internuclear distance in Fig. 2H with 2J, as indicated by arrows) and areas of multi-layered epithelium (arrowheads in Fig. 2J,K) were observed. The multilayering persisted in serial sections. Luminal cells were observed frequently within cysts (Fig. 2J,K).

p120ctn regulates tubule diameter

Immunofluorescence of sections from E17.5 control and mutant kidneys using a proximal tubule marker, lotus tetragonolobus lectin (LTL) showed that the cystic tubule regions were segments of proximal tubules (Fig. 3B,D). At higher magnification, there was increased diameter and decreased total length of mutant proximal tubules (Fig. 3C,D). Dilated tubules were noted as early as E15.5 (data not shown). Even tubules that were not overtly cystic had increased diameters. The cysts appeared only in proximal tubules; however, immunofluorescence with a distal tubule marker (sodium chloride co-transporter, NCC) showed a mild increase in distal tubule diameter (Fig. 3G,H). Visualization of thick ascending limb tubules using Tamm-Horsfall protein showed that they have normal diameters (Fig. 3I,J). Similarly, ureteric bud epithelia and collecting ducts were not dilated (Fig. 3E,F). These results indicate that the cystic defect in mutant kidneys is specific for proximal tubules.

Arvcf expression in developing nephrons

Lack of redundancy with a p120 homolog in proximal tubules is one possible explanation for the proximal tubule-specific cystogenesis. The localization of Arvcf, the closest p120ctn homolog, has been characterized in mature tubules (Walter et al., 2008). We extended this work by determining its distribution in developing kidneys. At E17.5 Arvcf was strongly expressed in ureteric bud, with lower expression in uncondensed and condensed mesenchyme (Fig. 1N; see Fig. S2 in the supplementary material). As the mesenchyme epithelialized, increased Arvcf was present in comma-shaped bodies (Fig. 1N). In the s-shaped bodies, Arvcf was

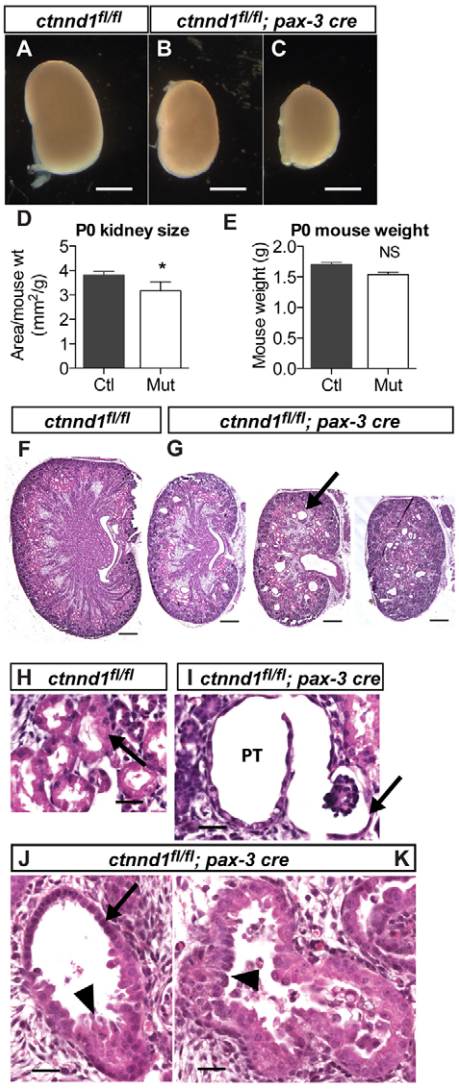

Fig. 2. p120ctn absence results in hypoplastic cystic kidneys. (**A-C**) Gross histology of P0 control (*ctnnd1*$^{flox/flox}$; A) and mutant (*ctnnd1*$^{flox/flox}$; *pax3-cre*$^{tg/0}$; B,C) mouse kidneys. (**D**,**E**) Quantification of differences between control and mutant in (D) renal size [kidney area (mm^2) per mouse weight (g)] $P<0.003$ and (E) P0 animal weight $P<0.10$. Data are mean ± s.d. Statistical analysis by the Mann-Whitney U-test. (**F**,**G**) Hematoxylin and Eosin (H&E)-stained sections from P0 control (F) and mutant (G) kidneys. Panels in G show sections from a single kidney with a cyst indicated (arrow). (**H-K**) Higher magnification images of H&E-stained cortex in control (H) and mutant (I-K) kidneys. I shows a cystic tubule involving Bowman's capsule (arrow) and proximal tubule (PT). J and K illustrate the most common morphologies observed: cuboidal epithelium with luminal cells and areas of multilayering (arrowheads). Arrows in H,J highlight the nuclear crowding in J compared with H. Scale bars: 1 mm in A-C; 250 μm in F,G; 25 μm in H-K.

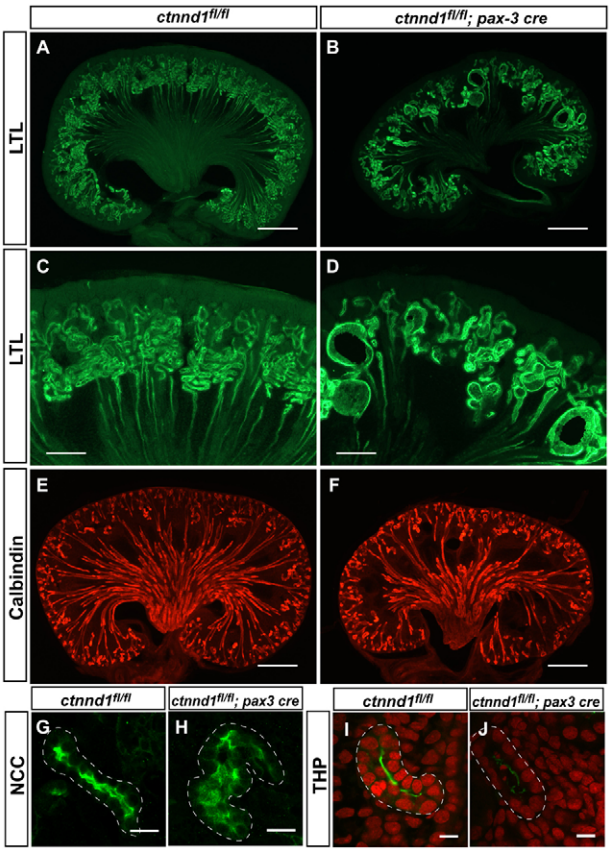

Fig. 3. p120ctn absence leads to proximal tubule cysts. (**A-D**) Visualization with a proximal tubule marker, LTL, in control (A,C) and mutant (B,D) mouse kidneys shows cysts and widened tubules. (**E**,**F**) Absence of cysts in ureteric bud and collecting ducts, identified by calbindin. (**G-J**) Mild luminal widening in mutant distal tubules, identified using anti-NaCl cotransporter (NCC; G,H) and absence of dilation in mutant thick ascending limb tubules, identified using anti-Tamm Horsfall Protein (I,J, dashed lines). Scale bars: 500 μm in A,B,E,F; 200 μm in C,D; 10 μm in G-J.

most abundant in the middle and distal regions (Fig. 1O). At E17.5, there was little or no Arvcf in proximal tubules (Fig. 1P), but it was present in loops of Henle (Fig. 1Q,R) and at low levels in distal tubules (Fig. 1S,T). This suggests that lack of Arvcf in embryonic proximal tubules might determine the proximal tubule-specificity of the cystic defects in p120ctn mutant kidneys. Similarly, the high Arvcf level in ureteric bud might explain why absence of p120ctn resulted in no obvious defects in this structure's derivatives. Of note, Arvcf was present in developing glomeruli (Fig. 1O) but, despite this, p120ctn mutant kidneys had obvious glomerular defects (see below). Another p120ctn homolog, δ-catenin, could not be detected by immunofluorescence in kidney, although the antibody strongly stained the brain (data not shown).

p120ctn maintains cadherin levels and is necessary for early tubulogenesis

To characterize the mechanisms that underlie cystogenesis, we first examined cadherin and catenin levels in control and mutant kidneys. Western blots of E17.5 kidney lysates showed that levels of R-cadherin, cadherin 11, E-cadherin, β-catenin and α-catenin were reduced globally (Fig. 4A,B). The level of active β-catenin, a marker for Wnt signaling, was similarly reduced. Interestingly, cadherin 6 was only mildly downregulated.

We next sought to determine whether the absence of p120ctn alters the distribution of individual cadherins. Immunofluorescence of cadherin 11 (Fig. 4M,R) showed that it was reduced in the mesenchyme of mutant mice. In renal vesicles, R-cadherin (not shown) and cadherin 6 were present in renal vesicles whereas E-cadherin was absent both in control and the p120ctn mutant (Fig. 4D,H, blue dotted lines and arrows indicate renal vesicles). The normal distributions of R-cadherin (not shown), cadherin 6 and E-cadherin in the proximal, mid and distal regions of the s-shaped body, respectively, were preserved in mutants in normally shaped s-shaped bodies (Fig. 4H, s-shaped body delineated by white dotted lines; compare with Fig. 4C). However, a significant number of abnormal comma or s-shaped bodies (10%; 4/40 s-shaped bodies) were also observed (arrowheads in Fig. 4I), and these showed disruption of the spatial distribution of cadherin 6 and E-cadherin (Fig. 4I-L, compare with 4D-G). Fig. 4L shows one such abnormal structure in which cadherin 6 positive cells (green) surround clustered E-cadherin- and cadherin 6-positive cells (arrow). The abnormal structures were visualized in their entirety by confocal microscopy to ensure that their abnormal appearance was not due to the plane of visualization. No similar structures were observed in control kidneys (0%; 0/35 s-shaped bodies). Examination of noncystic and cystic (data not shown) proximal tubules from p120ctn mutant mice showed that E-cadherin and β-catenin exhibited reduced expression levels, but maintained a normal basolateral distribution (Fig. 4N-Q,S-V,). Both R-cadherin and cadherin 6 were also present at low levels in proximal tubules, and R-cadherin levels were reduced considerably in mutants (data not shown).

Impaired fusion of the ureteric bud to mesenchymally derived epithelia might explain cyst formation once glomerular filtration becomes substantial (Mah et al., 2000). However, we found no difference in the percentage of fusions in control and p120ctn mutant kidneys (97% versus 95%; see Fig. S3 in the supplementary material).

p120ctn absence disrupts glomerular morphogenesis

As p120ctn is expressed in developing, but not mature, podocytes (data not shown) (Usui et al., 2003), we sought to determine whether its absence would affect glomerular morphogenesis. During early glomerulogenesis at the capillary loop stage, a single layer of developing podocytes from the proximal portion of the s-shaped body surrounds a forming capillary bed. As development proceeds, foot processes from podocytes extend to surround the lengthening capillaries. Each foot process is separated from another by a slit diaphragm, a modified adherens junction that allows selective filtration from capillaries.

Examination of mutant P0 kidneys using a glomerular marker, nephrin, revealed a normal glomerular density with a mild decrease in total glomerular number, consistent with reduced kidney size (Fig. 5A,E,X). At low magnification many, but not all, mutant glomeruli appeared smaller and less compact (Fig. 5B,F). At higher magnification, many of these glomeruli appeared disorganized with loss of podocyte and endothelial patterning (Fig. 5G,H, compare with 5C,D). Fig. 5G shows loss of contact between some podocytes and endothelial cells, whereas Fig. 5H shows podocytes that appear to be only minimally associated with neighboring podocytes.

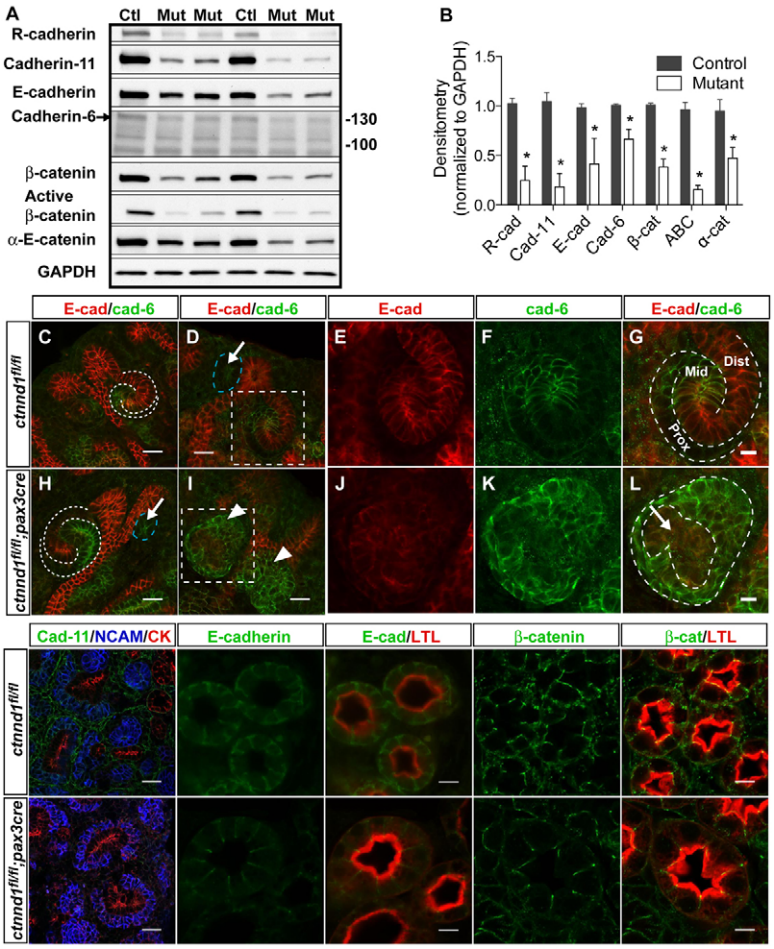

Fig. 4. Cadherins and catenins are downregulated dramatically in p120ctn mutant. (**A**) Western blots of cadherins and catenins from E17.5 control (Ctl) and mutant (Mut) mouse kidneys with GAPDH as a loading control. Active β-catenin is dephosphorylated Ser37/Thr41 (mAb 8E7) (van Noort et al., 2002). (**B**) Densitometry using ImageJ of cadherin and catenin levels normalized to GAPDH. n=5 for control (*ctnnd1*$^{flox/flox}$) and n=7 for mutant mice. Data are mean ± s.d. All decreased levels are statistically significant (Mann-Whitney U-test, P<0.005). (**C-L**) Localization of E-cadherin (red) and cadherin 6 (green) illustrates that cadherin 6 is present in control and mutant renal vesicles (D,H, blue dotted lines and arrows indicate renal vesicles). E-cadherin is in the distal s-shaped body, whereas cadherin 6 is in the mid-s-shaped body in control and mutant (C,H, white dotted lines delineate s-shaped bodies). Panel I shows two abnormal comma and s-shaped structures (arrowheads) in the mutant. Boxed area in D is shown at higher magnification in E-G. Boxed area in I is shown at higher magnification in J-L. (**M**,**R**) Localization of cadherin 11 (green), NCAM (blue) and cytokeratin (red, UB marker) shows loss of cadherin 11 from mesenchyme. (**N-Q**,**S-V**) Localization of E-cadherin (green, N,O,S,T), β-catenin (green, P,Q,U,V) and LTL (red, proximal tubule marker, O,T,Q,V) show reduced levels of E-cadherin and β-catenin in mutant proximal tubules. Scale bars: 25 μm in C,D,H,I; 10 μm in E-G,J-L,N-Q,S-V; 30 μm in M,R.

Examination of cadherins showed that R-cadherin, but not E- or P-cadherin (data not shown), is expressed in developing glomeruli, consistent with previous data (Goto et al., 1998). Cadherin 6 expression was limited to the surrounding parietal epithelial cells of Bowman's capsule (data not shown). In p120ctn mutants, R-cadherin levels were decreased dramatically in presumptive podocytes of developing glomeruli (Fig. 5I-M).

Examination of glomeruli revealed that the structural defect occurred early, at the capillary loop stage. In mutant mice, podocytes often did not completely surround the developing vasculature (Fig. 5V, compare with 5R). In some instances, the podocytes formed multiple rosettes (Fig. 5W) rather than a single oval sphere. Despite the morphological abnormalities and reduced R-cadherin, podocytes in p120ctn mutants developed slit-diaphragms, as evidenced by the podocin staining pattern in maturing glomeruli (Fig. 5O-Q,S-U).

p120ctn absence results in normal cell polarity but defective cytoskeletal organization

To determine whether absence of p120ctn resulted in cell polarity defects, we examined polarity marker distribution in proximal tubules. No differences between control and mutant in localizations of the basolateral marker Na/K ATPase (see Fig. S4A,B in the supplementary material), the apical marker lotus tetragonolobus lectin (Fig. 4O,Q,T,V) or the tight junction protein ZO1 (see Fig. S4C,D in the supplementary material) were observed. This indicates that despite low cadherin levels, p120ctn-null tubules maintain apical-basal polarity. However, we did note that mutant proximal tubules appeared to have increased apical actin filaments in noncystic proximal tubules (see Fig. S4H,G in the supplementary material) and dramatically increased actin bundles in cystic proximal tubules (see Fig. S4I in the supplementary material). This suggests that although gross apical-basolateral polarity is intact, there are abnormalities in cytoskeletal organization.

Absence of p120ctn increases proliferation in the proximal tubule

It has been suggested that increased proliferation contributes to renal cyst formation (Happe et al., 2009; Patel et al., 2008). Quantitative Western blot analysis showed that total proliferation was decreased within mutant kidneys (0.95±0.04 versus 0.60±0.09, P<0.02, Mann-Whitney U-test; see also Fig. S4J in the supplementary material), as expected given the renal hypoplasia. Analysis of proximal tubules showed that proliferation was increased twofold in the mutant (3.4±0.30 versus 7.3±0.67, P<0.006, Mann-Whitney U-test; see Fig. S4K in the supplementary material). Rates of apoptosis were low in mutant noncystic and cystic proximal tubules; however, there was a twofold increase in apoptosis in derivatives of metanephric mesenchyme, i.e. condensed mesenchyme, renal vesicles and comma and s-shaped bodies (P<0.03; see Fig. S4L in the supplementary material). To summarize, condensed mesenchyme and its derivatives displayed hypoplasia with increased apoptosis, whereas proximal tubules showed increased proliferation and cyst formation.

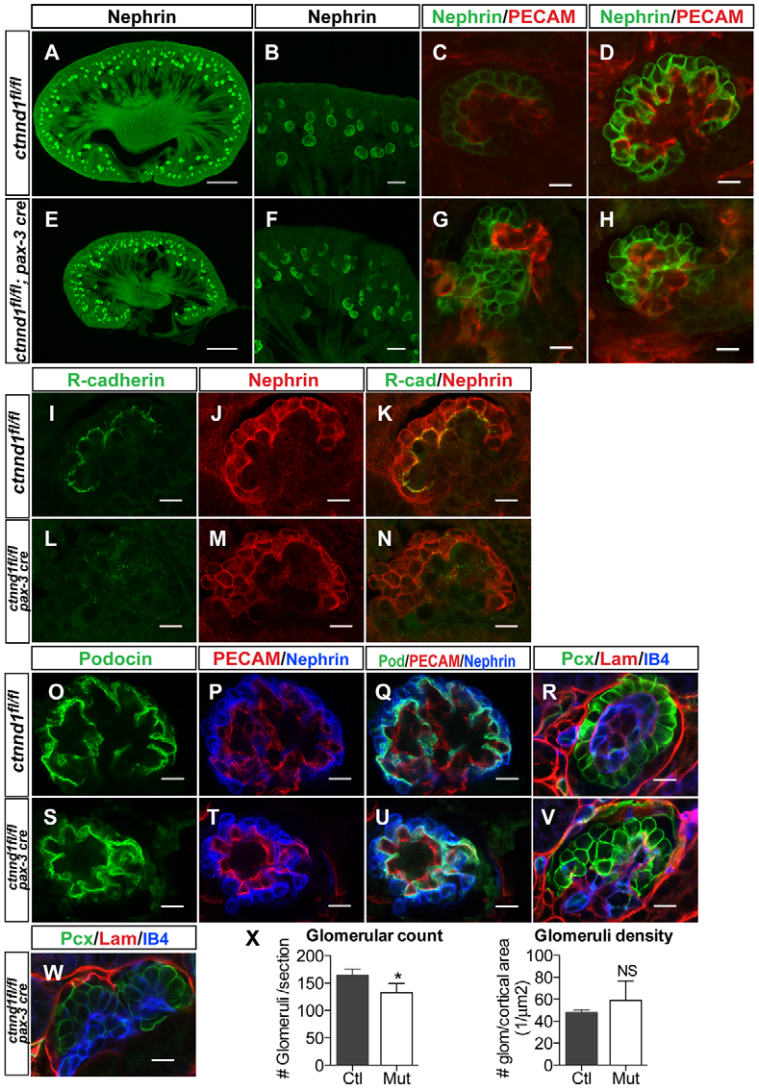

Fig. 5. p120ctn absence leads to defects in glomerulogenesis. (**A-H**) The podocyte marker nephrin (green) in P0 control (A,B) and mutant (E,F) mouse kidneys shows smaller, less compact glomeruli in the mutant. Anti-PECAM (red, C,D,G,H) identifies endothelial cells. (**I-N**) R-cadherin (green) and nephrin (red) in maturing glomeruli. R-cadherin is reduced in mutant presumptive podocytes. (**O-Q**,**S-U**) Localization of slit-diaphragm marker podocin (green), PECAM (red) and nephrin (blue). (**R**,**V**,**W**) Localization of podocyte marker podocalyxin (Pcx, green), endothelial marker IB4 (blue) and laminin (red) at the capillary loop stage at E17.5. (**X**) Quantification of glomerular number and glomerular density with ImageJ. *n*=4 embryos from three separate litters for each genotype. Data are mean ± s.d. There is a significant reduction in glomerular count ($P<0.03$) but not density ($P>0.50$). Mann-Whitney *U*-test. Scale bars: 500 µm in A,E; 100 µm in B,F; 10 µm C,D,G,H,I-W.

Mutations of numerous genes associated with cilia structure or formation have been associated with human polycystic kidney disease and murine models (Harris, 2009). Visualization of acetylated tubulin showed that the long slender cilia of proximal tubules appeared grossly normal in structure and number in noncystic proximal tubules from p120ctn mutants (see Fig. S5A,B in the supplementary material). The shape and length appeared abnormal in overtly cystic tubules (see Fig. S4C in the supplementary material), but this might be a secondary defect.

Mechanistic insights from 3D MDCK cell culture

To further characterize cyst formation in the absence of p120ctn, we stably depleted p120ctn in 3D MDCK cell cultures, which express isoform 3 (Ohkubo and Ozawa, 2004), via RNAi. Two different shRNA sequences (KD1 and KD2) substantially decreased p120ctn levels (Fig. 6B). Staining of knockdown cysts revealed very low levels of p120ctn (Fig. 6A) and substantially reduced E-cadherin (Fig. 6B,D). Notably, p120ctn knockdown did not reduce all cadherin levels equally; E-cadherin was substantially more reduced than cadherin 6 (85% versus 40%, respectively) (Fig. 6D), similar to in vivo observations (Fig. 4A,B). Thus, cadherins differ in their dependence on p120ctn in vivo and in vitro. As in vivo, intraluminal cells were observed in a large proportion of p120ctn knockdown cysts compared with controls (~60% versus ~10%, respectively) (Fig. 6A,E). Time-lapse microscopy demonstrated that luminal cells were extruded into the lumen from the cyst wall (data not shown). Rare p120ctn KD1 and KD2 cysts (0.5%), but not control cysts, showed areas of cellular multilayering (Fig. 6G, arrow), similar to observations in vivo. Furthermore, the size of knockdown cysts was visibly increased (Fig. 6F,G). By western blot, proliferation and apoptosis were increased in knockdown cysts (Fig. 6H,I). Localization of ZO1 (tight junction component), gm130 (Golgi marker) and podocalyxin (apical membrane marker) showed preserved cell polarity in the cyst wall (Fig. 6A,C,G). In summary, the p120ctn knockdown cysts had reduced cadherin levels, luminal cells, enlarged size and increased proliferation, rare multilayering of cells and preserved polarity. Our results show that p120ctn differentially stabilizes individual cadherins and demonstrate that MDCK cysts provide a relevant model for extending in vivo observations on p120ctn function in cystogenesis.

As depletion of p120ctn in both proximal tubules in vivo and MDCK cysts in vitro resulted in luminal extrusion of cells, we sought to determine whether loss of p120ctn resulted in reduced MDCK cell-cell adhesion. Ca^{2+}-dependent cell aggregation assays

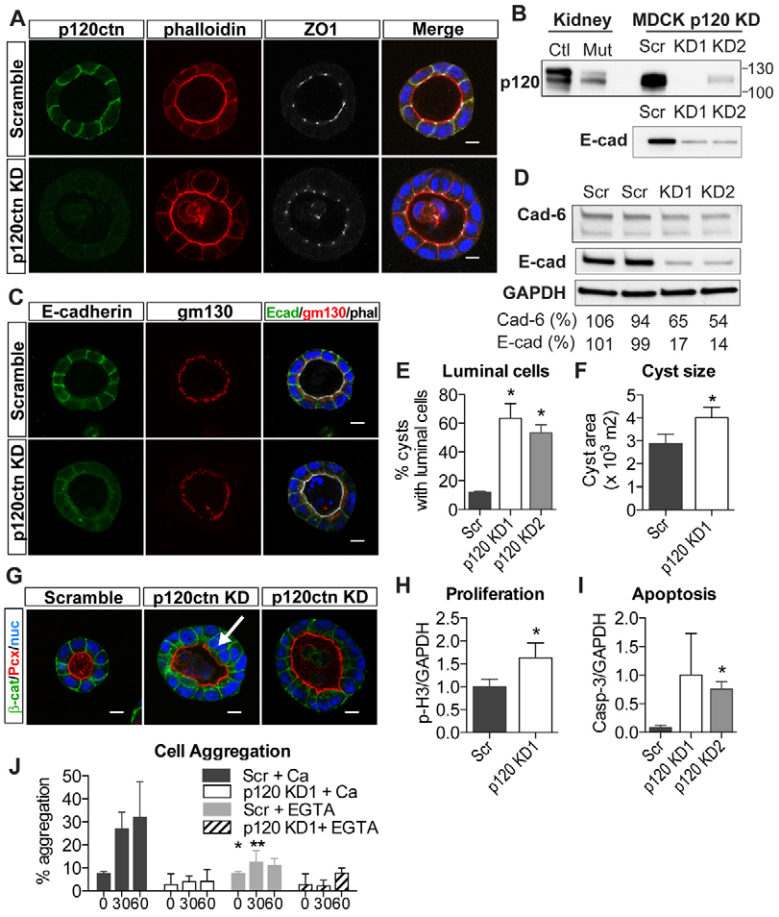

Fig. 6. p120 knockdown in 3D cyst culture results in enlarged cysts with reduced E-cadherin. (**A**,**C**) p120ctn and E-cadherin in p120ctn knockdown cysts. Panels show staining of phalloidin, ZO1 and gm130 as indicated. Merged images with Hoescht 33342 (blue, nuclei) show that p120 KD cysts contain intraluminal cells. (**B**) Western blot of p120ctn. Lanes 1 and 2: E17.5 kidney lysates from control and mutant. Lanes 3-5: MDCK cyst lysates from scramble and two p120 shRNA (KD1 and KD2). (**D**) Western blots of E-cadherin and cadherin 6 in control and p120ctn knockdown cysts. Percentages are E-cadherin and cadherin 6 levels normalized to GAPDH. (**E**) Quantification of percentage of cysts containing ≥1 luminal cell(s). Results are mean ± s.d. from three independent experiments with >300 cysts each (P<0.001 for scramble versus p120 KD1, and scramble versus p120 KD2). (**F**) Quantification of cyst area using DIC images analyzed in ImageJ. Results are mean ± s.d. of the upper quartile of cyst areas measured from three independent experiments done in triplicate with >300 cysts each (P<0.01 for scramble versus p120 KD1). (**G**) Localization of podocalyxin (Pcx, an apical membrane marker), β-catenin and Hoescht shows enlarged cysts and multilayered epithelium (arrow). (**H**,**I**) Densitometry of western blots of cyst lysates with phosphohistone-3 and active caspase-3 normalized to GAPDH. For phosphohistone-3, P<0.04 for scramble versus p120 KD1. For caspase-3, P<0.001 for scramble versus p120 KD2; P<0.09 scramble versus p120 KD1. (**J**) Cellular aggregation in scramble- and p120ctn-knockdown MDCK cells. Cells dissociated with EDTA were added to wells containing 1 mM $CaCl_2$ or 1 mM EGTA, and cellular aggregation assessed at times 0, 30 and 60 minutes. Percentage aggregation=(Na/N)×100 where Na=number of cells in aggregates ≥3 cells and N=total number of cells. Graph shows one of two similar experiments with three replicates for each time. Aggregation (mean ± s.d.) in p120ctn knockdown was reduced compared with control at 30 minutes (P<0.003) and 60 minutes (P<0.02). All statistical analysis was carried out using unpaired, two-tailed Student's t-test.

showed that dissociated p120ctn knockdown cells had a dramatically reduced ability to aggregate (Fig. 6J). Measurements of transepithelial resistance, a surrogate of tight junction integrity, in polarized monolayers showed that p120ctn knockdown monolayers had reduced resistance (see Fig. S6A in the supplementary material). In addition, confluent p120ctn knockdown cells appeared more elongated and mesenchyme-like (data not shown).

Another potential mechanism that might result in luminal cells in vivo and in vitro is altered orientation of cell division. The angle of cell division in proximal tubules is difficult to measure given the tubule tortuosity. We measured the spindle angle in the equatorial plane of control and p120ctn knockdown MDCK cysts and found no statistical differences (see Fig. S6B in the supplementary material). This suggests that misorientation of cell division does not contribute to the presence of luminal cells.

p120ctn has been shown to regulate the activities of Rho, Rac and Cdc42 (Anastasiadis et al., 2000; Noren et al., 2000; Wildenberg et al., 2006; Yanagisawa et al., 2008). In addition, inhibition of Rho kinase, a downstream effector of Rho, has been shown to cause defects in ureteric bud-derived tubulogenesis (Meyer et al., 2006; Michael et al., 2005). We performed GST-Rhotekin-RBD pulldown assays on MDCK cyst lysates and found a significant decrease in active GTP-bound RhoA in p120ctn knockdown cysts (Fig. 7A). Thus, absence of p120ctn isoform 3 appears to reduce RhoA activity in vitro.

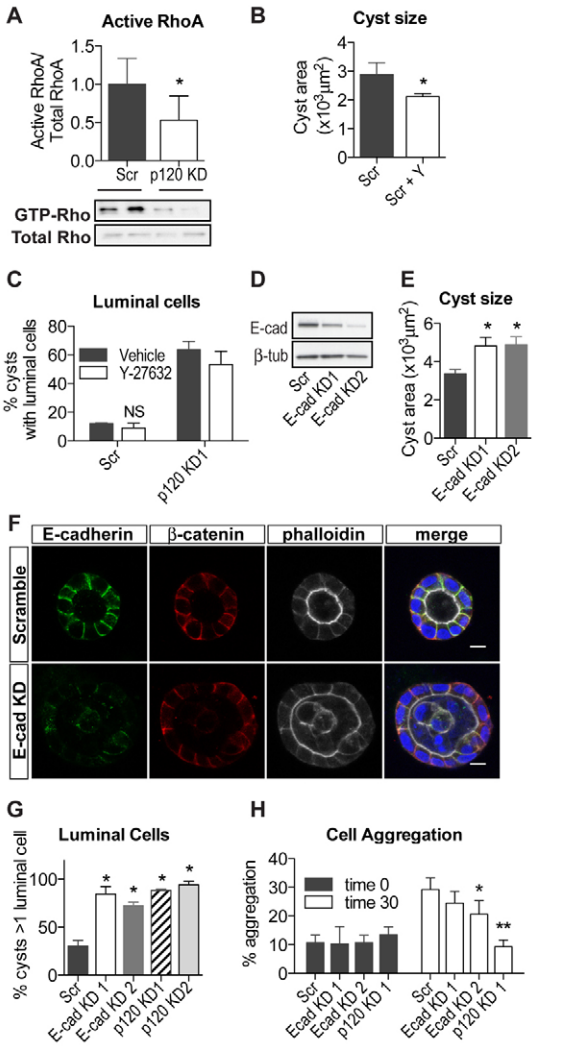

Fig. 7. E-cadherin knockdown but not RhoA inhibition phenocopies loss of p120ctn in MDCK cysts. (**A**) Rho activity assays. Quantification of GTP-Rho pull-downs using GST Rhotekin-RBD. GTP-Rho levels are normalized to total Rho. (**B**) Quantification of the effect of ROCK inhibition (Y-27632, 10 μM) on cyst area using DIC images analyzed in ImageJ. Results are mean ± s.d. of the upper quartile of cyst areas. Cysts treated with Y-27632 are smaller than control (P<0.03). (**C**) Quantification of the effect of ROCK inhibitor (Y-27632, 10 μM) on the percentage of cysts with luminal cells (P<0.4 for scramble versus scramble +Y-27632). (**D**) Western blot of E-cadherin from MDCK lysates with scramble or two E-cadherin shRNA (KD1 and KD2). (**E**) Quantification of cyst area performed as described for panel B (P<0.001 for scramble versus E-cadherin KD1 or KD2). (**F**) Visualization of E-cadherin reduction in E-cadherin KD cysts. Panels show β-catenin and phalloidin as indicated. Merged images with Hoescht 33342 (blue, nuclei) show intraluminal cells in E-cadherin KD cysts. (**G**) Quantification of percentage of cysts containing >1 luminal cell (P<0.001 for scramble versus each KD). (**H**) Cellular aggregation in scramble, E-cadherin KD and p120 KD cells. Cells dissociated with EDTA were added to wells containing 1 mM $CaCl_2$ and cellular aggregation assessed at 0 and 30 minutes. Percentage aggregation was determined as described for Fig. 6J. Graph shows one of two similar experiments with four replicates for each time (P<0.15 for scramble versus E-cadherin KD1; P<0.03 for scramble versus E-cadherin KD2; P<0.001 for scramble versus p120 KD1, all at 30 minutes). All graphical results are mean ± s.d. and were analyzed with an unpaired two-tailed Student's t-test. Panels B,C,E and G are from three independent experiments done in triplicate with >300 cysts each.

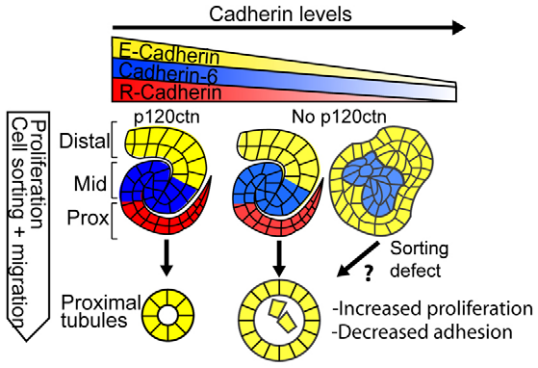

Fig. 8. Proposed model of p120ctn function in renal tubulogenesis. p120ctn maintains cadherin levels for appropriate migration and/or sorting of cells in renal vesicles into the distinct domains of comma- and s-shaped bodies. In the absence of p120ctn, cadherin levels are reduced, with a fraction of the vesicles failing to form normal s-shaped bodies. As the s-shaped body elongates into tubules, p120 regulates proliferation and migration.

To determine whether reduced active RhoA plays a role in the p120ctn-knockdown phenotype, we treated control cysts with a Rho kinase (ROCK) inhibitor Y-27632. This did not result in increased cyst size (Fig. 7B) or intraluminal cell number (Fig. 7C). Thus, decreased RhoA signaling is unlikely to underlie the defects observed with p120ctn deficiency.

To determine whether the cystic abnormalities resulting from p120ctn deficiency might be caused by reduced cadherin levels, we examined the structures of E-cadherin-deficient cysts, prepared by stable E-cadherin knockdown (Fig. 7D,E). These cysts were enlarged (Fig. 7E,F) and contained many luminal cells (Fig. 7F,G). Furthermore, E-cadherin knockdown also resulted in reduced cellular aggregation (Fig. 7H). Together, these results suggest that E-cadherin deficiency, and not RhoA inhibition, underlies the defects in the p120ctn mutant cysts and suggest that cadherin loss is responsible for the phenotypes observed in vivo.

DISCUSSION

Our data demonstrates that p120ctn absence in the metanephric mesenchyme leads to hypoplastic kidneys with defective tubular and glomerular morphogenesis. Furthermore, p120ctn is required for establishing a normal lumen diameter and for preventing cyst formation within proximal tubules. Similarly, p120ctn knockdown in 3D MDCK cells results in enlarged and abnormal cysts. Delaminated cells are observed in both the mutant proximal tubules and p120ctn-knockdown MDCK cysts. p120ctn knockdown in MDCK cells results in decreased Ca^{2+}-dependent cellular aggregation and loss of tight junction integrity, demonstrating in vitro that, in renal epithelial cells, p120ctn is required for normal intercellular adhesion. Both in vivo and in vitro, p120ctn deficiency results in reduced cadherin levels. This might be the central event in causing cystogenesis and cell delamination in vivo, because E-cadherin knockdown partially phenocopies loss of p120ctn in vitro.

Although p120ctn deficiency in proximal tubules manifests as cystic tubules, in other tubule segments loss of p120ctn does not lead to a severe phenotype. Several lines of evidence suggest that functional redundancy of p120ctn and Arvcf might account for this result. Collectively, p120ctn family members control cadherin levels in a dose-dependent manner (Xiao et al., 2003), and Arvcf expression can functionally substitute for p120ctn in vitro (Davis

et al., 2003). Thus, differing levels of Arvcf might partially explain why absence of p120ctn results in a segment-specific phenotype, in addition to other contributing factors, such as the unique cell type, the individual cadherins expressed and the total cellular cadherin level. We observed that Arvcf levels are high in ureteric buds and loops of Henle, and absence of p120ctn does not result in a discernible phenotype. Likewise, Arvcf is undetectable in proximal tubules and absence of p120ctn results in proximal tubule cytogenesis. In the cap mesenchyme, podocyte precursors and distal tubules, Arvcf expression is modest, leading to phenotypes of varying severity. Whether this is due to Arvcf substituting for p120ctn or due to complex cellular differences remains unknown.

From our results, we propose a model (Fig. 8) in which the absence of p120ctn, through reduced cadherin levels, leads to early defects in migration and/or aggregation of cell types (cellular sorting) within s-shaped bodies. The presence of ~10% abnormal structures in mutant s-shaped bodies suggests that there might be a cadherin threshold for these defects, with only the lowest levels resulting in defective s-shaped organization. Although p120ctn family members have not yet been shown to play a crucial role in cellular segregation and sorting, a role for cadherins in cell segregation has been well documented in the central nervous system (Inoue et al., 2001; Price et al., 2002).

Intriguingly, our data show that some cadherins are more sensitive than others to absence of p120ctn. Data from cell mixing studies demonstrate that differences in cadherin levels can promote cell sorting (Duguay et al., 2003). Differences in the reduction of different cadherins might, thus, cause the disorganized s-shaped bodies observed in p120ctn mutants. As the s-shaped bodies subsequently undergo proliferation, migration and differentiation to form mature tubule segments, p120ctn may additionally regulate both proliferation and migration with its absence resulting in hyperproliferative cystic proximal tubules.

Our data suggest that increased tubule diameter in the p120ctn mutant might be the result of several defects. We show that absence of p120ctn results in excessive proliferation in proximal tubular epithelium, despite overall renal hypoplasia. In addition, p120ctn depletion from MDCK cysts also leads to hyperproliferation. Recent data suggests that increased proliferation enhances cyst formation (Happe et al., 2009; Patel et al., 2008). Prior work has shown that p120ctn isoforms 1 and 3 inhibit cell proliferation in various cell types (Liu et al., 2009; Soto et al., 2008; Wildenberg et al., 2006). These increases may be mediated by the reductions in cadherins, as suggested by the enlarged E-cadherin knockdown cysts. E-cadherin has been shown to inhibit cell growth (Perrais et al., 2007) and may do so in a p120ctn-dependent manner (Soto et al., 2008).

Absence of p120ctn might cause abnormal tubular and glomerular phenotypes because of aberrant cell movements during tubule elongation and glomerular morphogenesis. It has been proposed that convergent extension-like processes regulate tubule elongation and diameter (Karner et al., 2009). Depletion of *Xenopus* p120ctn results in defective convergent-extension of ectoderm explants as well as abnormal morphogenetic movements in gastrulation and axial elongation (Ciesiolka et al., 2004; Fang et al., 2004). Prior studies conducted in mammalian mesenchymal cell lines show that p120ctn regulates cell migration (Boguslavsky et al., 2007; Yanagisawa et al., 2008), and that this is dependent on p120ctn's interactions with cadherins (Yanagisawa and Anastasiadis, 2006).

The presence of luminal cells within p120ctn-deficient proximal tubules and MDCK cysts suggests the possibility of a cell adhesion defect. Supportive of this, our data show that dissociated cells from p120ctn knockdown MDCK cells exhibit decreased Ca^{2+}-dependent aggregation. Further, p120ctn knockdown results in reduced integrity of the intercellular barrier formed by tight junctions, as recently shown also in a colon cancer line (Smalley-Freed et al., 2010). As with proliferation defects, the decreased cellular adhesion may be due to reductions in surface cadherin(s) as E-cadherin knockdown also results in reduced adhesion. In summary, we have shown that p120ctn is crucial for normal tubular and glomerular development probably by modulating cell surface cadherins.

Acknowledgements

We thank Keling Zang for technical assistance; Michael Shiloh, Rana Datta, James Linton, Tom Carroll and Hui-Teng Cheng for advice; the UCSF Small Molecule Discovery Center for use of the IN Cell Analyzer 1000; Jonathan Epstein and Andrew McMahon for mice; and Gregory Dressler, James Nelson, Mechthild Hatzfeld, Tom Jessell, Bruce Stevenson, Peter Mundel, Lawrence Holzman and Al Reynolds for antibodies. This work was supported by the National Kidney Foundation Young Investigator Grant (D.K.M.), March of Dimes (P.R.B.) and NIH grants DK081668, DK068358, DK074398, DK067153, and DK064338. Deposited in PMC for release after 12 months.

Competing interests statement

The authors declare no competing financial interests.

Supplementary material

Supplementary material for this article is available at
http://dev.biologists.org/lookup/suppl/doi:10.1242/dev.056564/-/DC1

References

Aho, S., Levansuo, L., Montonen, O., Kari, C., Rodeck, U. and Uitto, J. (2002). Specific sequences in p120ctn determine subcellular distribution of its multiple isoforms involved in cellular adhesion of normal and malignant epithelial cells. *J. Cell Sci.* **115**, 1391-1402.

Anastasiadis, P. Z., Moon, S. Y., Thoreson, M. A., Mariner, D. J., Crawford, H. C., Zheng, Y. and Reynolds, A. B. (2000). Inhibition of RhoA by p120 catenin. *Nat. Cell Biol.* **2**, 637-644.

Boguslavsky, S., Grosheva, I., Landau, E., Shtutman, M., Cohen, M., Arnold, K., Feinstein, E., Geiger, B. and Bershadsky, A. (2007). p120 catenin regulates lamellipodial dynamics and cell adhesion in cooperation with cortactin. *Proc. Natl. Acad. Sci. USA* **104**, 10882-10887.

Brakeman, P. R., Liu, K. D., Shimizu, K., Takai, Y. and Mostov, K. E. (2009). Nectin proteins are expressed at early stages of nephrogenesis and play a role in renal epithelial cell morphogenesis. *Am. J. Physiol. Renal Physiol.* **296**, F564-F574.

Bryant, D. M., Datta, A., Rodriguez-Fraticelli, A. E., Peranen, J., Martin-Belmonte, F. and Mostov, K. E. (2010). A molecular network for de novo generation of the apical surface and lumen. *Nat. Cell Biol.* **12**, 1035-1045.

Capaldo, C. T. and Macara, I. G. (2007). Depletion of E-cadherin disrupts establishment but not maintenance of cell junctions in Madin-Darby canine kidney epithelial cells. *Mol. Biol. Cell* **18**, 189-200.

Cheng, H. T., Kim, M., Valerius, M. T., Surendran, K., Schuster-Gossler, K., Gossler, A., McMahon, A. P. and Kopan, R. (2007). Notch2, but not Notch1, is required for proximal fate acquisition in the mammalian nephron. *Development* **134**, 801-811.

Chiasson, C. M., Wittich, K. B., Vincent, P. A., Faundez, V. and Kowalczyk, A. P. (2009). p120-catenin inhibits VE-cadherin internalization through a Rho-independent mechanism. *Mol. Biol. Cell* **20**, 1970-1980.

Cho, E. A. and Dressler, G. R. (2003). Formation and development of nephrons. In *The Kidney: From Normal Development to Congenital Disease* (ed. P. D. Vize, A. S. Woolf and J. Bard), pp. 195-208. Amsterdam and Boston: Academic Press.

Cho, E. A., Patterson, L. T., Brookhiser, W. T., Mah, S., Kintner, C. and Dressler, G. R. (1998). Differential expression and function of cadherin-6 during renal epithelium development. *Development* **125**, 803-812.

Ciesiolka, M., Delvaeye, M., Van Imschoot, G., Verschuere, V., McCrea, P., van Roy, F. and Vleminckx, K. (2004). p120 catenin is required for morphogenetic movements involved in the formation of the eyes and the craniofacial skeleton in Xenopus. *J. Cell Sci.* **117**, 4325-4339.

Dahl, U., Sjodin, A., Larue, L., Radice, G. L., Cajander, S., Takeichi, M., Kemler, R. and Semb, H. (2002). Genetic dissection of cadherin function during nephrogenesis. *Mol. Cell. Biol.* **22**, 1474-1487.

Davis, M. A. and Reynolds, A. B. (2006). Blocked acinar development, E-cadherin reduction, and intraepithelial neoplasia upon ablation of p120-catenin in the mouse salivary gland. *Dev. Cell* **10**, 21-31.
Davis, M. A., Ireton, R. C. and Reynolds, A. B. (2003). A core function for p120-catenin in cadherin turnover. *J. Cell Biol.* **163**, 525-534.
Dressler, G. R. (2009). Advances in early kidney specification, development and patterning. *Development* **136**, 3863-3874.
Duguay, D., Foty, R. A. and Steinberg, M. S. (2003). Cadherin-mediated cell adhesion and tissue segregation: qualitative and quantitative determinants. *Dev. Biol.* **253**, 309-323.
Elia, L. P., Yamamoto, M., Zang, K. and Reichardt, L. F. (2006). p120 catenin regulates dendritic spine and synapse development through Rho-family GTPases and cadherins. *Neuron* **51**, 43-56.
Fang, X., Ji, H., Kim, S. W., Park, J. I., Vaught, T. G., Anastasiadis, P. Z., Ciesiolka, M. and McCrea, P. D. (2004). Vertebrate development requires ARVCF and p120 catenins and their interplay with RhoA and Rac. *J. Cell Biol.* **165**, 87-98.
Golenhofen, N. and Drenckhahn, D. (2000). The catenin, p120ctn, is a common membrane-associated protein in various epithelial and non-epithelial cells and tissues. *Histochem. Cell Biol.* **114**, 147-155.
Goto, S., Yaoita, E., Matsunami, H., Kondo, D., Yamamoto, T., Kawasaki, K., Arakawa, M. and Kihara, I. (1998). Involvement of R-cadherin in the early stage of glomerulogenesis. *J. Am. Soc. Nephrol.* **9**, 1234-1241.
Grieshammer, U., Cebrian, C., Ilagan, R., Meyers, E., Herzlinger, D. and Martin, G. R. (2005). FGF8 is required for cell survival at distinct stages of nephrogenesis and for regulation of gene expression in nascent nephrons. *Development* **132**, 3847-3857.
Gumbiner, B. M. (2005). Regulation of cadherin-mediated adhesion in morphogenesis. *Nat. Rev. Mol. Cell Biol.* **6**, 622-634.
Halbleib, J. M. and Nelson, W. J. (2006). Cadherins in development: cell adhesion, sorting, and tissue morphogenesis. *Genes Dev.* **20**, 3199-3214.
Happe, H., Leonhard, W. N., van der Wal, A., van de Water, B., Lantinga-van Leeuwen, I. S., Breuning, M. H., de Heer, E. and Peters, D. J. (2009). Toxic tubular injury in kidneys from Pkd1-deletion mice accelerates cystogenesis accompanied by dysregulated planar cell polarity and canonical Wnt signaling pathways. *Hum. Mol. Genet.* **18**, 2532-2542.
Harris, P. C. (2009). 2008 Homer W. Smith award: insights into the pathogenesis of polycystic kidney disease from gene discovery. *J. Am. Soc. Nephrol.* **20**, 1188-1198.
Inoue, T., Tanaka, T., Takeichi, M., Chisaka, O., Nakamura, S. and Osumi, N. (2001). Role of cadherins in maintaining the compartment boundary between the cortex and striatum during development. *Development* **128**, 561-569.
Karner, C. M., Chirumamilla, R., Aoki, S., Igarashi, P., Wallingford, J. B. and Carroll, T. J. (2009). Wnt9b signaling regulates planar cell polarity and kidney tubule morphogenesis. *Nat. Genet.* **41**, 793-799.
Keirsebilck, A., Bonne, S., Staes, K., van Hengel, J., Nollet, F., Reynolds, A. and van Roy, F. (1998). Molecular cloning of the human p120ctn catenin gene (CTNND1): expression of multiple alternatively spliced isoforms. *Genomics* **50**, 129-146.
Li, J., Chen, F. and Epstein, J. A. (2000). Neural crest expression of Cre recombinase directed by the proximal Pax3 promoter in transgenic mice. *Genesis* **26**, 162-164.
Liu, Y., Dong, Q. Z., Zhao, Y., Dong, X. J., Miao, Y., Dai, S. D., Yang, Z. Q., Zhang, D., Wang, Y., Li, Q. C. et al. (2009). P120-catenin isoforms 1A and 3A differently affect invasion and proliferation of lung cancer cells. *Exp. Cell Res.* **315**, 890-898.
Mah, S. P., Saueressig, H., Goulding, M., Kintner, C. and Dressler, G. R. (2000). Kidney development in cadherin-6 mutants: delayed mesenchyme-to-epithelial conversion and loss of nephrons. *Dev. Biol.* **223**, 38-53.
McCrea, P. D. and Park, J. I. (2007). Developmental functions of the P120-catenin sub-family. *Biochim. Biophys. Acta* **1773**, 17-33.
Meyer, T. N., Schwesinger, C., Sampogna, R. V., Vaughn, D. A., Stuart, R. O., Steer, D. L., Bush, K. T. and Nigam, S. K. (2006). Rho kinase acts at separate steps in ureteric bud and metanephric mesenchyme morphogenesis during kidney development. *Differentiation* **74**, 638-647.
Michael, L., Sweeney, D. E. and Davies, J. A. (2005). A role for microfilament-based contraction in branching morphogenesis of the ureteric bud. *Kidney Int.* **68**, 2010-2018.
Mo, Y. Y. and Reynolds, A. B. (1996). Identification of murine p120 isoforms and heterogeneous expression of p120cas isoforms in human tumor cell lines. *Cancer Res.* **56**, 2633-2640.
Montonen, O., Aho, M., Uitto, J. and Aho, S. (2001). Tissue distribution and cell type-specific expression of p120ctn isoforms. *J. Histochem. Cytochem.* **49**, 1487-1496.
Noren, N. K., Liu, B. P., Burridge, K. and Kreft, B. (2000). p120 catenin regulates the actin cytoskeleton via Rho family GTPases. *J. Cell Biol.* **150**, 567-580.
Oas, R. G., Xiao, K., Summers, S., Wittich, K. B., Chiasson, C. M., Martin, W. D., Grossniklaus, H. E., Vincent, P. A., Reynolds, A. B. and Kowalczyk, A. P. (2010). p120-catenin is required for mouse vascular development. *Circ. Res.* **106**, 941-951.
Ohkubo, T. and Ozawa, M. (2004). The transcription factor Snail downregulates the tight junction components independently of E-cadherin downregulation. *J. Cell Sci.* **117**, 1675-1685.
Park, J. S., Valerius, M. T. and McMahon, A. P. (2007). Wnt/beta-catenin signaling regulates nephron induction during mouse kidney development. *Development* **134**, 2533-2539.
Patel, V., Li, L., Cobo-Stark, P., Shao, X., Somlo, S., Lin, F. and Igarashi, P. (2008). Acute kidney injury and aberrant planar cell polarity induce cyst formation in mice lacking renal cilia. *Hum. Mol. Genet.* **17**, 1578-1590.
Perez-Moreno, M., Davis, M. A., Wong, E., Pasolli, H. A., Reynolds, A. B. and Fuchs, E. (2006). p120-catenin mediates inflammatory responses in the skin. *Cell* **124**, 631-644.
Perrais, M., Chen, X., Perez-Moreno, M. and Gumbiner, B. M. (2007). E-cadherin homophilic ligation inhibits cell growth and epidermal growth factor receptor signaling independently of other cell interactions. *Mol. Biol. Cell* **18**, 2013-2025.
Price, S. R., De Marco Garcia, N. V., Ranscht, B. and Jessell, T. M. (2002). Regulation of motor neuron pool sorting by differential expression of type II cadherins. *Cell* **109**, 205-216.
Reynolds, A. B. (2007). p120-catenin: past and present. *Biochim. Biophys. Acta* **1773**, 2-7.
Saxen, L. and Sariola, H. (1987). Early organogenesis of the kidney. *Pediatr. Nephrol.* **1**, 385-392.
Schmidt-Ott, K. M. and Barasch, J. (2008). WNT/beta-catenin signaling in nephron progenitors and their epithelial progeny. *Kidney Int.* **74**, 1004-1008.
Smalley-Freed, W. G., Efimov, A., Burnett, P. E., Short, S. P., Davis, M. A., Gumucio, D. L., Washington, M. K., Coffey, R. J. and Reynolds, A. B. (2010). p120-catenin is essential for maintenance of barrier function and intestinal homeostasis in mice. *J. Clin. Invest.* **120**, 1824-1835.
Soto, E., Yanagisawa, M., Marlow, L. A., Copland, J. A., Perez, E. A. and Anastasiadis, P. Z. (2008). p120 catenin induces opposing effects on tumor cell growth depending on E-cadherin expression. *J. Cell Biol.* **183**, 737-749.
Srinivas, S., Goldberg, M. R., Watanabe, T., D'Agati, V., al-Awqati, Q. and Costantini, F. (1999). Expression of green fluorescent protein in the ureteric bud of transgenic mice: a new tool for the analysis of ureteric bud morphogenesis. *Dev. Genet.* **24**, 241-251.
Usui, J., Kurihara, H., Shu, Y., Tomari, S., Kanemoto, K., Koyama, A., Sakai, T., Takahashi, T. and Nagata, M. (2003). Localization of intercellular adherens junction protein p120 catenin during podocyte differentiation. *Anat. Embryol. (Berl.)* **206**, 175-184.
van Noort, M., Meeldijk, J., van der Zee, R., Destree, O. and Clevers, H. (2002). Wnt signaling controls the phosphorylation status of beta-catenin. *J. Biol. Chem.* **277**, 17901-17905.
Walter, B., Schlechter, T., Hergt, M., Berger, I. and Hofmann, I. (2008). Differential expression pattern of protein ARVCF in nephron segments of human and mouse kidney. *Histochem. Cell Biol.* **130**, 943-956.
Wildenberg, G. A., Dohn, M. R., Carnahan, R. H., Davis, M. A., Lobdell, N. A., Settleman, J. and Reynolds, A. B. (2006). p120-catenin and p190RhoGAP regulate cell-cell adhesion by coordinating antagonism between Rac and Rho. *Cell* **127**, 1027-1039.
Xiao, K., Allison, D. F., Buckley, K. M., Kottke, M. D., Vincent, P. A., Faundez, V. and Kowalczyk, A. P. (2003). Cellular levels of p120 catenin function as a set point for cadherin expression levels in microvascular endothelial cells. *J. Cell Biol.* **163**, 535-545.
Xiao, K., Garner, J., Buckley, K. M., Vincent, P. A., Chiasson, C. M., Dejana, E., Faundez, V. and Kowalczyk, A. P. (2005). p120-Catenin regulates clathrin-dependent endocytosis of VE-cadherin. *Mol. Biol. Cell* **16**, 5141-5151.
Yanagisawa, M. and Anastasiadis, P. Z. (2006). p120 catenin is essential for mesenchymal cadherin-mediated regulation of cell motility and invasiveness. *J. Cell Biol.* **174**, 1087-1096.
Yanagisawa, M., Huveldt, D., Kreinest, P., Lohse, C. M., Cheville, J. C., Parker, A. S., Copland, J. A. and Anastasiadis, P. Z. (2008). A p120 catenin isoform switch affects Rho activity, induces tumor cell invasion, and predicts metastatic disease. *J. Biol. Chem.* **283**, 18344-18354.
Yu, J., Carroll, T. J. and McMahon, A. P. (2002). Sonic hedgehog regulates proliferation and differentiation of mesenchymal cells in the mouse metanephric kidney. *Development* **129**, 5301-5312.